Journal of Solid State Chemistry **163,** 144–150 (2002)
doi:10.1006/jssc.2001.9385, available online at http://www.idealibrary.com on IDEAL®

Structure and Ionic Conductivity of $Bi_6Cr_2O_{15}$, a New Structure Type Containing $(Bi_{12}O_{14})_n^{8n+}$ Columns and CrO_4^{2-} Tetrahedra

J. Grins,*,[1] S. Esmaeilzadeh,* and S. Hull†

*Department of Inorganic Chemistry, Arrhenius Laboratory, Stockholm University, SE-106 91 Stockholm, Sweden; and †The ISIS Facility, Rutherford Appleton Laboratory, Oxfordshire OX11 0QX, U.K.

Received June 5, 2001; accepted August 30, 2001

Powder samples of the Cr^{6+}-containing compound $Bi_6Cr_2O_{15}$ were prepared by solid state reaction of Bi_2O_3 and Cr_2O_3 in air at 650°C. The structure was solved and refined using high-resolution neutron powder diffraction data in space group *Ccc*2, with anisotropic thermal displacement parameters $a = 12.30184(5)$, $b = 19.87492(7)$, and $c = 5.88162(2)$ Å, $V = 1438.0$ Å^3, and 126 variables to $R_F = 1.8\%$. $Bi_6Cr_2O_{15}$ exhibits a new structure type that contains $(Bi_{12}O_{14})_n^{8n+}$ columns, of the kind previously found only for phases isotypic with $Bi_{13}Mo_4VO_{34}$. Each column is surrounded by eight CrO_4^{2-} tetrahedra. The ionic conductivity of $Bi_6Cr_2O_{15}$ was determined by impedance measurements to be 3.5×10^{-5} $(\Omega\,\mathrm{cm})^{-1}$ at 600°C. © 2002 Elsevier Science

Key Words: **bismuth; chromium; $Bi_6Cr_2O_{15}$; crystal structure; neutron diffraction; ionic conductivity.**

INTRODUCTION

Bismuth-based oxides have been studied extensively for a number of potentially useful physical properties: oxygen ion conductivity (1, 2), ferroelectricity (3), and superconductivity (4). Applications have also been found for Bi–Mo oxides as catalysts for selective oxidation and ammoxidation of olefins (5).

The crystal structures of bismuth-based oxides are often complex and have for many phases not yet been determined, even for cases where single crystals are available, partly due to the difficulty in determining O atom positions from X-ray data. The majority of the bismuth-rich compounds in the systems Bi–*M*–O (*M* = V, Nb, Ta, Mo, W) have fluorite-related structures and they exhibit a variety of superstructures and/or commensurate and incommensurate modulations (6–11).

Vannier *et al.* reported in 1996 a monoclinic solid solution with a new and unique structure type in the system Bi_2O_3–MoO_3–V_2O_5 (12). The end-members were given as $Bi_{26}Mo_{10}O_{69}$ and $Bi_{26}Mo_9VO_{67}$. The structure contains $(Bi_{12}O_{14})_\infty$ columns that are separated by (Mo/V)O_4 tetrahedra and isolated Bi atoms. The derived structure model has ideally 68 O atoms per formula unit and the apparent necessity to either remove or insert O atoms in the structure was not resolved. A year later, Enjalbert *et al.* stated that oxygen nonstoichiometry is not possible, neither in the columns nor in the tetrahedra, and that the correct composition for the V-containing phase is $Bi_{26}Mo_8V_2O_{68}$ ($Bi_{13}Mo_4VO_{34}$) (13). Possible replacement mechanisms were, however, envisaged that allow for an isotypic phase in the pure Bi_2O_3–MoO_3 system, with a metal composition of 22.2–25.9% Mo. Subsequent studies have shown the existence of other isotypic column phases: $PbBi_{12}Mo_5O_{34}$ (14) and $Bi(Bi_{12-x}Te_xO_{14})Mo_{4-x}V_{1+x}O_{20}$ $(0 \le x \le 2.5)$ (15). The space group symmetry for the latter phase is, at the specific composition with $x = 1$, lowered from centric $P2/c$ to acentric $P2$, with an associated halving of the *c*-axis. It is a very good oxygen ion conductor with $\sigma = 8.0 \times 10^{-3}$ $(\Omega\,\mathrm{cm})^{-1}$ at 750°C (16, 17).

In comparison with, e.g., the Bi–Mo–O system, the Bi-rich side of the Bi–Cr–O system has been less investigated. The deep red and Cr^{6+}-containing compound $Bi_{14}CrO_{24}$ has a tetragonal ($I4/m$) structure with CrO_4^{2-} tetrahedra occupying large cages (18). We have characterized, by electron microscopy and X-ray diffraction, a high-temperature solid solution $Bi_{1-x}Cr_xO_{1.5+1.5x}$, $0.05 \le x \le 0.15$, that exhibits a 3-D incommensurate modulation (19). The title compound $Bi_6Cr_2O_{15}$ was synthesized and its structure determined as a part of studying the Bi–Cr–O system. We have in this system found a set of other phases that are under current investigation, including one that has been previously observed (18), with ~16% Cr and a large fluorite superstructure with $a \approx 3a_F$, $b \approx 5a_F$, $c \approx 3a_F$.

EXPERIMENTAL

Powder samples of $Bi_6Cr_2O_{15}$ were prepared by solid state reaction of Bi_2O_3 (Strem Chemicals, 99.999%) and

[1] To whom correspondence should be addressed. Fax: +46 8 15 21 87. E-mail: mat@inorg.su.se.

0022-4596/02 $35.00

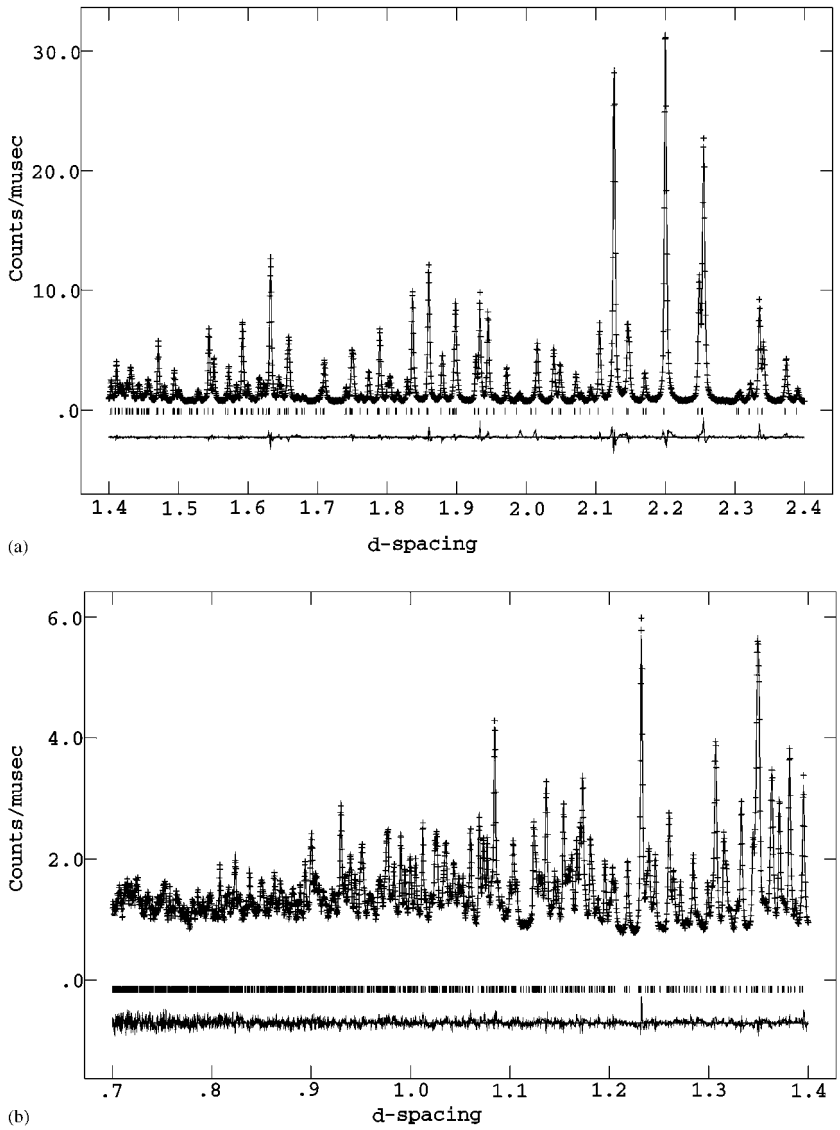

FIG. 1. Observed (crosses), calculated (solid line), and difference (bottom) TOF NPD pattern of $Bi_6Cr_2O_{15}$ for (a) $d = 1.4$–2.4 Å and (b) 0.7–1.4 Å.

Cr_2O_3 (Strem Chemicals, 99.999%) at 650°C. Pelleted samples were heat-treated three times for 72 h, with intermediate regrindings, and then rapidly cooled to room temperature.

The phase purity of the samples was checked by X-ray powder diffraction (XRPD) with a Guinier-Hägg camera, using Cu$K\alpha_1$ radiation. XRPD data for partial structure solution were also recorded for $2\theta = 10$–$130°$ with a STOE STADI/P diffractometer, with Cu$K\alpha_1$ radiation, a small position-sensitive detector covering 4.6°, and the sample in symmetric transmission mode.

The metal composition was found to agree with the nominal one of 25% Cr using energy-dispersive X-ray analysis in a JEOL JSM 880 scanning electron microscope.

Time-of-flight neutron powder diffraction (NPD) data were collected on the high-resolution diffractometer at the UK spallation neutron source ISIS, Rutherford Appleton Laboratory. The Rietveld structure refinements were made with the GSAS program (20).

Two-terminal measurements of the ionic conductivity were performed using pelleted samples of $\sim$6 mm diameter and $\sim$6 mm length. These were held between two spring-loaded platinum discs inside a boron nitride cell which was inserted into a horizontal tube furnace. Details of the measuring cell can be obtained elsewhere (21). Complex-impedance measurements were performed approximately every 3 min while the furnace temperature was ramped up, then down, at 60 K h^{-1}. The maximum temperature used

TABLE 1
Atomic Parameters for $Bi_6Cr_2O_{15}$: Orthorhombic, $a = 12.30184(5)$, $b = 19.87492(7)$, $c = 5.88162(2)$ Å, $V = 1438.0$ Å^3, $Ccc2$, $Z = 4$

Atom	Site	x	y	z	$U_{eq}/(Å^2 \times 100)$
Bi1	8*d*	0.1088(2)	0.0650(1)	0.2336(3)	1.62
Bi2	8*d*	0.1019(1)	0.2011(1)	0.8266(4)	1.58
Bi3	8*d*	0.3209(1)	0.0668(1)	0.8290(4)	1.50
Cr	8*d*	0.3667(4)	0.1642(2)	0.3499(11)	2.23
O1	8*d*	0.2534(2)	0.0007(2)	0.0940(6)	1.84
O2	8*d*	0.0086(3)	0.1561(1)	0.1037(6)	1.86
O3	8*d*	0.8435(2)	0.0962(2)	0.3829(5)	1.80
O4	4*a*	0	0	0.0579(7)	1.66
O5	8*d*	0.3097(3)	0.1758(2)	0.1030(5)	3.79
O6	8*d*	0.2725(3)	0.1599(2)	0.5563(6)	3.43
O7	8*d*	0.4292(2)	0.0912(2)	0.3447(8)	4.32
O8	8*d*	0.4516(3)	0.2241(2)	0.4149(5)	4.76

Anisotropic Thermal Displacement Parameters ($Å^2 \times 100$), Defined by $T = \exp([-2\pi^2(h^2a^{*2}U_{11} + \ldots 2hka^*b^*U_{12}\ldots)]$

Atom	U_{11}	U_{22}	U_{33}	U_{12}	U_{13}	U_{23}
Bi1	2.0(10)	1.92(11)	0.94(9)	0.07(10)	− 0.06(9)	0.19(9)
Bi2	1.55(10)	1.28(9)	1.92(10)	− 0.03(7)	0.61(12)	0.03(10)
Bi3	1.43(10)	1.61(10)	1.45(9)	− 0.16(7)	− 0.07(11)	− 0.25(13)
Cr	1.87(21)	2.28(20)	2.55(22)	− 0.27(21)	0.78(25)	0.31(29)
O1	2.04(16)	1.93(16)	1.56(15)	0.48(18)	0.31(17)	0.32(12)
O2	2.18(17)	1.85(15)	1.56(16)	− 0.02(16)	0.56(12)	0.34(15)
O3	1.31(17)	2.01(15)	2.09(19)	− 0.62(12)	0.74(13)	0.37(13)
O4	1.26(19)	1.44(20)	2.27(27)	− 0.78(23)	0	0
O5	4.37(23)	4.76(25)	2.25(18)	0.25(18)	− 0.98(20)	0.03(18)
O6	3.39(23)	3.26(23)	3.65(23)	0.48(16)	1.40(17)	0.78(17)
O7	3.89(21)	3.24(21)	5.81(21)	0.29(14)	0.56(25)	0.14(22)
O8	5.38(26)	4.50(21)	4.42(25)	− 3.39(18)	0.77(17)	− 1.03(18)

was ~875 K. A Solartron S1260 frequency response analyzer determined the conventional Z–Z' Bode plot over the frequency range from 0.1 Hz to 10 MHz. The real component of the sample impedance Z_S was determined using the program IMMFIT (21). All measurements were performed in air and temperature monitoring was achieved using chromel/alumel thermocouples located ~2 mm from the sample pellet.

RESULTS

Structure Determination and Refinement

The XRPD pattern of $Bi_6Cr_2O_{15}$ was indexed using a C-centered orthorhombic unit cell with unit cell parameters, finally refined from the NPD data, $a = 12.30184(5)$, $b = 19.87492(7)$, and $c = 5.88162(2)$ Å, $V = 1438.0$ Å^3. Systematic absent reflections (hkl: $h + k \neq 2n$; $0kl$: k, $l \neq 2n$; $h0l$: h, $l \neq 2n$) implied the diffraction symbol Ccc and the two possible space groups $Ccc2$ and $Cccm$. Positions for the Bi atoms could, however, not be located from the X-ray data using either of these two space group. They were derived using the monoclinic space group Cc and the direct methods program EXPO for powder data (22). The Bi atom positions showed that the structure is fluorite related, with $a \approx 2a_F$, $b \approx 4a_F$, and $c \approx a_F$, and strongly indicated $(Bi_{12}O_{14})_\infty$ columns of the kind found for $Bi_{13}Mo_4VO_{34}$ (13). Reliable O atom positions could not be determined from the XRPD data. The correct space group $Ccc2$ and the O atom positions were found by using the NPD data and difference Fourier maps. In the final refinement, anisotropic thermal displacement parameters were used for all atoms, 1171 reflections for $d = 0.7$–2.5 Å, and 126 variables (33 positional and 70 thermal displacement parameters). The refinement converged with $\chi^2 = 3.1$, $wR_p = 3.9\%$, $R_p = 3.4\%$, $Dwd = 0.72$, and $R_F = 1.8\%$. The fit between observed and calculated patterns is shown in Fig. 1. Obtained atomic parameters are given in Table 1 and selected bond distances in Table 2. A simultaneous use of neutron and X-ray data yielded no apparent improvement in determined parameters, a total $\chi^2 = 4.4$, and $R_F = 2.9\%$ and 2.7%, respectively.

Structure Description

The structure is illustrated in Fig. 2. It contains $(Bi_{12}O_{14})_n^{8n+}$ columns, along the twofold axes at $0, 0, z$ and $\frac{1}{2}, \frac{1}{2}, z$. The columns are separated by CrO_4^{2+} tetrahedra with each column surrounded by eight tetrahedra. A separate column is illustrated from a side view in Fig. 3. The Bi1 atoms, in the inner part of the columns, are coordinated by four O atoms at 2.13–2.34 Å, with the Bi(III) lone pair E completing a distorted trigonal bipyramid BiO_4E. Approximate directions of the lone pair E can be obtained from valence vectors (23) $\Phi_i = -\sum_j \phi_{ij}$. Each vector ϕ_{ij} is directed from the Bi atom i to the ligand O atom j and has a length $|\phi_{ij}| = \exp(-d_{ij}/0.2)$. Accordingly, the lone pairs for the Bi1 atoms are directed nearly parallel with the column, at an angle of ~20°, as illustrated in Fig. 3. The Bi2 and Bi3 atoms, on the column periphery, are coordinated by three O atoms at 2.09–2.21 Å. Their lone pairs complete BiO_3E tetrahedra and are directed perpendicular to the column, at an angle of ~3° with the ab plane. The

TABLE 2
Bond Distances (Å) for $Bi_6Cr_2O_{15}$

Bi1–O1	2.340(4)	Bi2–O2	2.089(4)	Bi3–O1	2.096(4)
O2	2.319(4)	O2	2.184(4)	O1	2.201(4)
O3	2.232(3)	O3	2.215(3)	O3	2.129(3)
O4	2.128(3)	O8	2.429(4)	O6	2.520(4)
O4	2.664(4)	O6	2.757(3)		
		O8	2.917(4)		
Cr–O5	1.629(7)				
O6	1.680(7)				
O7	1.642(6)				
O8	1.630(5)				

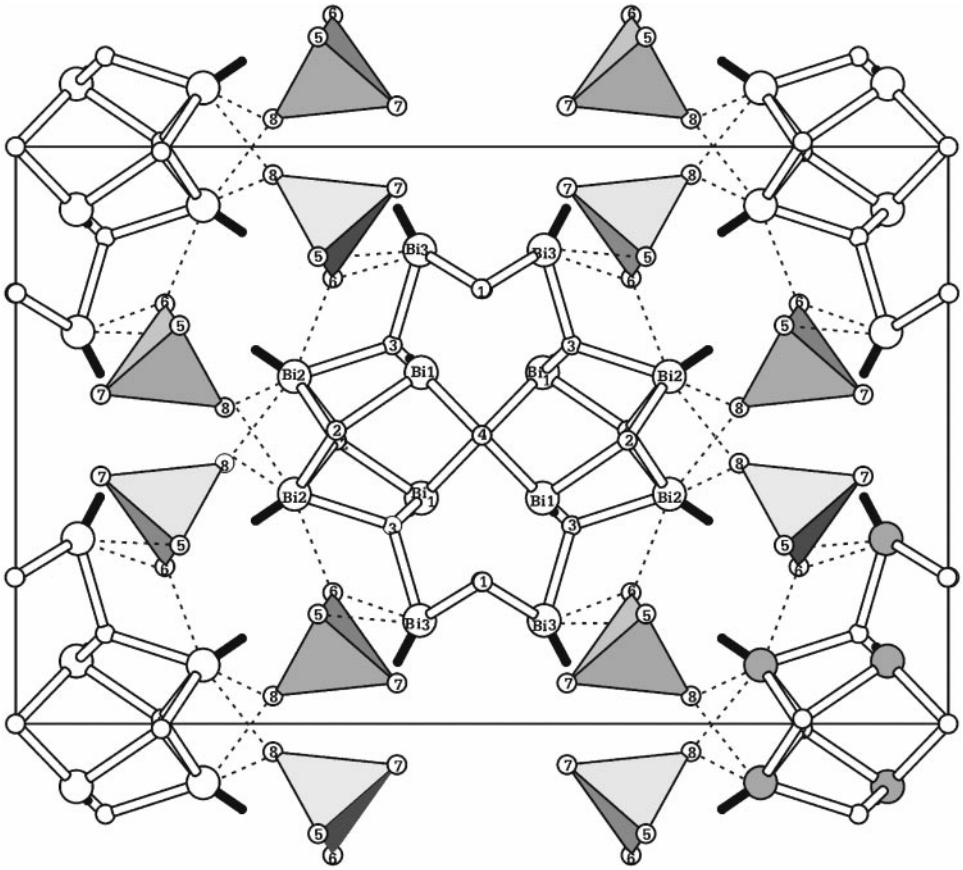

FIG. 2. The structure of $Bi_6Cr_2O_{15}$ projected on the *xy* plane. The atoms are numbered in accordance with Table 1. Short (≤ 2.23 Å) and long (> 2.23 and ≤ 2.92 Å) Bi–O bonds are shown by spokes and dotted lines, respectively. The black rods illustrate approximate locations of the Bi lone electron pairs.

Bi2 and Bi3 atoms are also weakly bonded to three of the four O atoms of the CrO_4 tetrahedra at 2.43–2.92 Å (see Fig. 2). The CrO_4 tetrahedron is almost regular with d(Cr–O) 1.63–1.68 Å. The mean Cr–O distance 1.645 Å is nearly identical with the mean Cr–O bond length 1.647 Å in α-K_2CrO_4 (24).

Valence bond sums (VBSs) (25) calculated from $VBS_i = \sum_j v_{ij}$ with $v_{ij} = \exp[(R_0 - d_{ij})/0.37]$ and R_0(Bi–O) = 2.904 Å, R_0(Cr–O) = 1.794 Å gives + 5.99 for Cr and + 2.87, + 3.20, and + 3.16 for Bi1–Bi3, respectively, including in the calculations Bi–O distances up to 3 Å. The corresponding VBSs for the O atoms vary between − 1.88 and − 2.32, with the exception of O7 which has a very low VBS of − 1.51. This low value is a direct consequence of O7 being only bonded to Cr at 1.642(6) Å. The agreement of the VBSs for the Bi atoms with the formal valence of + 3 improves if corrections for the stereochemical effect of the lone pair are applied according to the formula proposed by Wang and Liebau (23), yielding VBSs of + 2.99, + 2.89, and + 3.07, including here in the calculations only the three or four shortest Bi–O distances.

Ionic Conductivity

The frequency dependence of the impedance was measured between 560 and 885 K in a heating–cooling cycle. The ion conductivity was calculated from the intercept of the semicircular arcs obtained in complex impedance plots. Figure 4 shows the logarithm of the conductivity $\log(\sigma)$ as a function of the inverse temperature $1/T$. $Bi_6Cr_2O_{15}$ is found to be a moderate oxygen ion conductor with 3.5×10^{-5} $(\Omega\,\text{cm})^{-1}$ at 873 K. The conductivity does not follow an Arrhenius-type behavior $\log(\sigma) \propto 1/T$ over the entire temperature interval. The curvature in the plot may be due to a temperature dependence of the activation energy, e.g., $E_a = E_{a0} - E_{a1} \cdot T^2$, or to different conduction mechanisms dominating at lower and higher temperatures. The curve can, however, be approximated rather well by a straight line for $T \geq 740$ K, with a corresponding activation energy of 1.54 eV.

DISCUSSION

The structure of $Bi_6Cr_2O_{15}$ is a new type of column structure. Isolated $(Bi_{12}O_{14})_n^{8n+}$ columns have previously

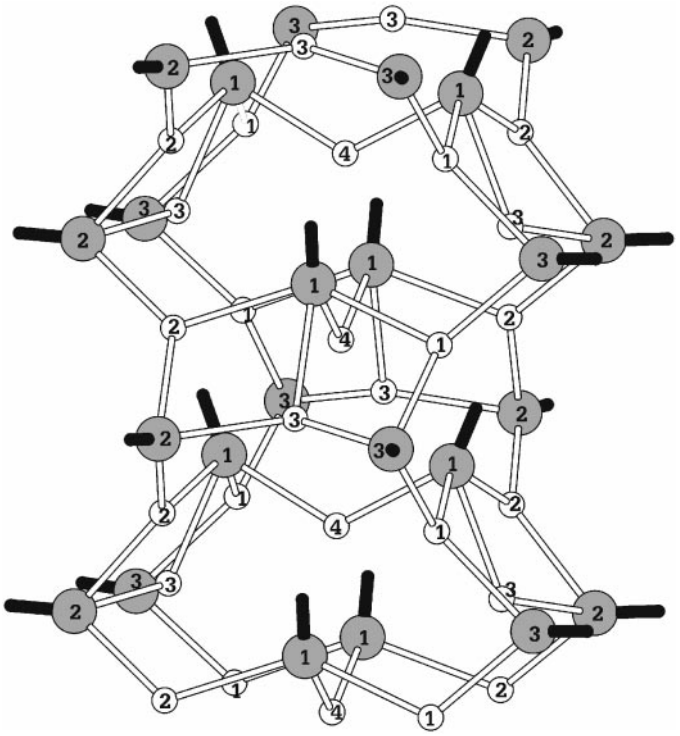

FIG. 3. A side view of a $(Bi_{12}O_{14})_n^{8n+}$ column. The atoms are numbered in accordance with Table 1. Bi and O atoms with bonds ≤ 2.23 Å are connected. The black rods illustrate approximate locations of the Bi lone electron pairs.

been found only for $Bi_{13}Mo_4VO_{34}$ (12, 13) and isotypic phases (14, 15). $Bi_{13}Mo_4VO_{34}$ crystallizes in space group $P2/c$ with $a = 11.652(7)$, $b = 5.7923(8)$, and $c = 24.420(9)$ Å, $\beta = 101.38(6)^\circ$ (13). The structure, illustrated in Fig. 5a, can

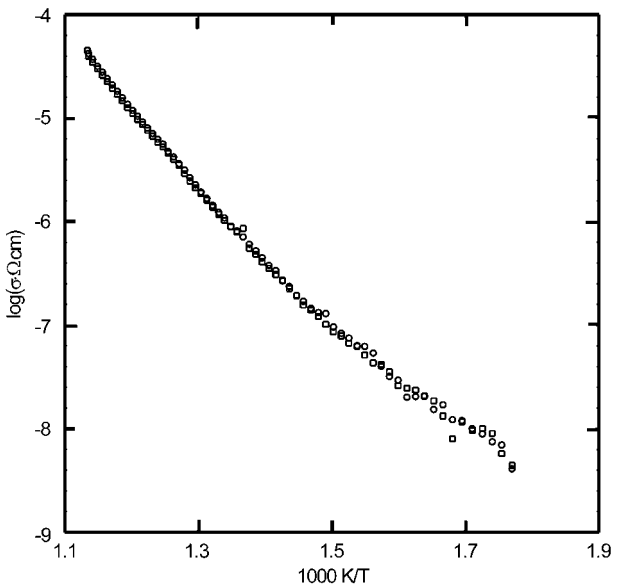

FIG. 4. Conductivity Arrhenius plot.

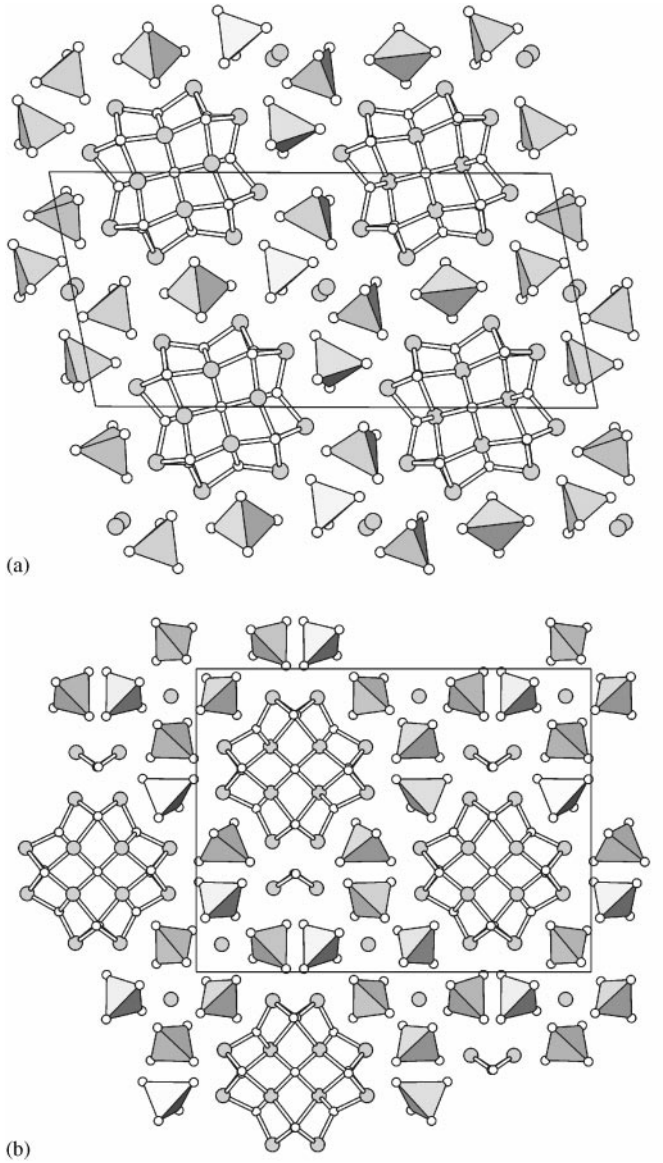

FIG. 5. The structures of (a) $Bi_{13}Mo_4VO_{34}$, projected on the xz plane, and (b) γ(H)-Bi_2MoO_6, projected on the xy plane. Bi and O atoms are illustrated by larger shaded and smaller unfilled circles, respectively.

be compared with that of $Bi_6Cr_2O_{15}$ (Fig. 2). For the comparison the stoichiometries may be written as respectively $Bi_2[Bi_{12}O_{14}]_2[MO_4]_{10}$ (M = Mo/V) and $[Bi_{12}O_{14}]_2$ $[MO_4]_8$ (M = Cr). The former phase has a higher M metal content, 27.7% compared with 25%. Each column is in the structure surrounded by 10 tetrahedra, compared with 8 for $Bi_6Cr_2O_{15}$, and there are two additional noncolumn Bi atoms per formula unit, located on partially occupied sites that are surrounded by six MO_4 tetrahedra. Accompanying the disorder for the additional Bi atoms, the O atoms of the MO_4 tetrahedra are found to have very high thermal displacement parameters (12, 13, 15),

or to partially occupy sites that form a distorted cube (14). The thermal displacement parameters for the O atoms of the CrO_4 tetrahedra for $Bi_6Cr_2O_{15}$ are, in contrast, found to be significantly smaller and do not show any significant anisotropy.

The two types of column structures are similar to those of γ(H)-Bi_2MoO_6 (26) and substituted homologues (27). γ(H)-Bi_2MoO_6 crystallizes in space group $P2_1/c$ with $a = 17.2627(1)$, $b = 22.4296(2)$, and $c = 5.58489(5)$ Å and $\beta = 90.4974(6)^\circ$ (26). The structure is illustrated in Fig. 5b. It contains $(Bi_{12}O_{14})_n^{8n+}$ columns with adjacent parallel Bi_2O_2 chains, forming together "Latin cross" columns $(Bi_2O_2)\cdot(Bi_{12}O_{14})_n^{10n+}$, with the Bi_2O_2 chains constituting the foot of the cross. Each "Latin cross" column is surrounded by 14 MoO_4 tetrahedra. In addition, there are four noncolumn Bi atoms per unit cell, each surrounded by four MoO_4 tetrahedra. A structure-oriented formula for γ(H)-Bi_2MoO_6 can accordingly be written as $Bi_4[Bi_2O_2][Bi_{12}O_{14}]_2[MO_4]_{16}$ (M = Mo).

The compound $Bi_6Cr_2O_{15}$ could be expected to be a good oxygen ion conductor, in view of its structural similarity to the solid solution $Bi(Bi_{12-x}Te_xO_{14})Mo_{4-x}V_{1+x}O_{20}$ ($0 \le x \le 2.5$) (15), which exhibits a conductivity as high as $\sigma = 8.0 \times 10^{-3}$ $(\Omega\,\mathrm{cm})^{-1}$ at 750°C ($x = 1$) with an activation energy $E_a = 0.84$ eV (16, 17). It is, however, found to be a considerably more modest oxygen ion conductor. It is speculative to attribute this to any structural difference between the phases, but it seems to imply that a high oxygen ion mobility in column phases is not provided solely by the presence of the columns, but depends significantly on the atoms and their arrangement between the columns.

The conduction mechanism in the column phases is furthermore not known, e.g., if the moving species are interstitials or vacancies, and the structures do, a priori, not appear to allow oxygen nonstoichiometry (13), neither in the columns nor in the tetrahedra. It has been proposed (28) that for Bi_2O_3-based ionic conductors, in general, the migration pathways are close to the locations of the lone pairs, because these are the most polarizable part of the Bi atom coordination sphere and the structures are in these parts also less occupied by atoms than other parts. In this context, the atom configuration for $Bi_6Cr_2O_{15}$ around the twofold axis at $0, \frac{1}{2}, z$ is intriguing. As shown in Fig. 2, the space around this axis is very empty. The O7 atoms around the axis are bonded only to Cr atoms and the distance between two O7 atoms with the same z coordinate is 4.0 Å. If the lone pairs are assumed to be located ~ 1 Å from the Bi atoms, then those for Bi3 are at positions corresponding to the O7 atom positions, but displaced by $\frac{1}{2}$ along the c-axis. These lone pair regions would appear to make suitable zig-zag migration pathways for oxygen ions along the c-axis. This conjecture is, however, not confirmed by the measured conductivity, which is not very high.

While Bi-rich oxides containing such elements as V, W, Mo, Nb, or Ta are usually yellow, Bi–Cr phases have been noted for their orange to red colors (18, 19). The optical absorption has the characteristics of charge transfer bands. In the case of the deep red compound $Bi_{14}CrO_{24}$, the charge transfer process has been proposed to occur between Bi^{3+} and Cr^{6+} via interconnecting O atoms (18). We could neither reject nor confirm this postulate, an alternative being electronic transitions from the ligand O atoms to Cr, for $Bi_{1-x}Cr_xO_{1.5+1.5x}$ (19). The compound $Bi_6Cr_2O_{15}$ is bright yellow, in contrast to the usual orange-red colors of Bi–Cr oxides with 5–20% Cr. It also shows a marked change in color with temperature, the color changing from bright yellow at room temperature, via orange and red, to a deep brown at 650°C. These color changes are very rapid, as a quick removal of a powder sample from a hot-plate shows, and are therefore unlikely to originate from impurities or compositional changes. Thermogravimetric measurements did not show any weight changes of $Bi_6Cr_2O_{15}$ upon heating in air to 650°C. Preliminary high-temperature XRPD data, collected with a STOE image plate Guinier-Hägg camera, revealed furthermore no change in structure or appearance of additional reflections at temperatures below 650°C. Further studies of the "thermochromic" properties of $Bi_6Cr_2O_{15}$ are scheduled.

ACKNOWLEDGMENTS

We thank Dr. K. Knight at ISIS for his generous and invaluable help with the neutron data collection and Prof. M. Nygren for support and valuable discussions. This work has been financially supported by the Swedish Natural Science Foundation.

REFERENCES

1. J. C. Boivin and G. Mairesse, *Chem. Mater.* **10,** 2870 (1998).
2. K. R. Kendall, C. Navas, J. K. Thomas, and H.-C. zur Loye, *Chem. Mater.* **8,** 642 (1996).
3. E. L. Subbarao, *J. Phys. Chem. Solids*, **23,** 665 (1962).
4. R. J. Cava, B. Batlogg, J. J. Krajewski, R. Farrow, L. W. Rupp, Jr., A. E. White, K. Short, W. F. Peck, and T. V. Kometani, *Nature* **332,** 814 (1988).
5. R. K. Graselli, *J. Chem. Educ.* **63,** 216 (1986).
6. A. Castro, E. Aguado, J. M. Rojo, P. Herrero, R. Enjalbert, and J. Galy, *Mater. Res. Bull.* **33**(1), 31 (1998).
7. C. E. Infante, C. Gronemeyer, and F. Li, *Solid State Ionics* **25,** 63 (1987).
8. W. Zhou, *J. Solid State Chem.* **108,** 381 (1994).
9. M. Valldor, S. Esmaeilzadeh, C. Pay-Gomez, and J. Grins, *J. Solid State Chem.* **152,** 573 (2000).
10. W. Zhou, *J. Solid State Chem.* **87,** 44 (1990).
11. W. Zhou, *J. Solid State Chem.* **101,** 1 (1992).
12. R. N. Vannier, G. Mairesse, F. Abraham, and G. Nowogrocki, *J. Solid State Chem.* **122,** 394 (1996).
13. R. Enjalbert, G. Hasselmann, and J. Galy, *J. Solid State Chem.* **131,** 236 (1997).

14. R. Enjalbert, G. Hasselmann, and J. Galy, *Acta Crystallogr. Sect. C* **53,** 269 (1997).
15. A. Castro, R. Enjalbert, P. Baules, and J. Galy, *J. Solid State Chem.* **139,** 185 (1998).
16. J. Galy, R. Enjalbert, A. Castro, and P. Millet, *SPIE Int. Conf. Solid Crystals* **3724,** 86 (1998).
17. P. Begue, J. M. Rojo, R. Enjalbert, J. Galy, and A. Castro, *Solid State Ionics* **112,** 275 (1998).
18. S. A. Warda, W. Pietzuch, W. Massa, U. Kesper, and D. Reinen, *J. Solid State Chem.* **149,** 209 (2000).
19. S. Esmaeilzadeh, S. Lundgren, U. Hålenius, and J. Grins, *J. Solid State Chem.* **156,** 168 (2001).
20. A. C. Larson and R. B. Von Dreele, Los Alamos National Laboratory Report No. LA-UR-86-748, 1987.
21. N. J. G. Gardner, S. Hull, D. A. Keen, and P. Berastegui, Rutherford Appleton Laboratory Report RAL-TR-1988-032, 1998.
22. A. Altomare, M. C. Burla, M. Camalli, B. Carrozzini, G. L. Cascarano, C. Giacovazzo, A. Guagliardi, A. G. G. Moliterni, G. Polidori, and R. Rizzi, *J. Appl. Crystallogr.* **32**(2), 339 (1999).
23. X. Wang and F. Liebau, *Z. Kristallogr.* **211,** 437 (1996).
24. K. Toriumi and Y. Saito, *Acta Crystallogr. Sect. B* **34,** 3149 (1978).
25. I. D. Brown and D. Altermatt, *Acta Crystallogr. Sect. B* **41,** 244 (1985).
26. D. J. Buttrey, T. Vogt, U. Wildgruber, and W. R. Robinson, *J. Solid State Chem.* **111,** 118 (1994).
27. P. Bégué, R. Enjalbert, J. Galy, and A. Castro, *Solid State Sci.* **2,** 637 (2000).
28. A. Laarif and F. Theobald, *Solid State Ionics* **21,** 183 (1986).